A R C H I V E S O F M E T A L L U R G Y A N D M A T E R I A L S
Volume 59 2014 Issue 1
DOI: 10.2478/amm-2014-0004

Z. AHMADIAN*, I. DANAEE*, M.A. GOLOZAR**

EFFECT OF SURFACE TREATMENT ON CORROSION RESISTANCE OF 304 STAINLESS STEEL IMPLANTS IN TYRODE SOLUTION

WPŁYW OBRÓBKI POWIERZCHNIOWEJ NA ODPORNOŚĆ NA KOROZJĘ IMPLANTÓW ZE STALI NIERDZEWNEJ 304 W PŁYNIE TYRODE'A

The effect of different surface preparation methods such as mechanical, chemical and electrochemical surface preparation on the formation, stability and deterioration of surface films formed on austenitic 304 stainless steel was investigated in Tyrode's physiological solution by cyclic polarization curves, AC impedance measurements surface techniques. A hysteresis loop in a cyclic polarization curve was obtained that indicates a delay in repassivation of an existing pit when the potential is scanned cathodically. Electrolytic polishing and ultrasonic cleaning improves corrosion resistance by increasing the value of the corrosion potential and breakdown potential of the passive layer as well as the pit initiation potential. After mechanical polishing no perfect passivation region was observed. Change in surface fractal is in good agreement with the result obtained from height roughness factor of AFM.

Keywords: Electrolytic polishing, Chemical passivation, 304 Stainless steel, AFM

Wpływ różnych sposobów przygotowania powierzchni, takich jak mechaniczne, chemiczne i elektrochemiczne na tworzenie, stabilność i degradację warstw powierzchniowych utworzonych na austenitycznej stali nierdzewnej 304, badano w fizjologicznym płynie Tyrode'a technikami badań powierzchni – cyklicznych krzywych polaryzacyjnych oraz impedancji. Uzyskano pętlę histerezy cyklicznej krzywej polaryzacyjnej, co wskazuje na opóźnienie w repasywacji istniejących wżerów podczas skanowania potencjału w kierunku katodowym. Elektrolityczne polerowanie i czyszczenie ultradźwiękowe poprawia odporność korozyjną poprzez zwiększenie potencjału korozyjnego i potencjału przebicia warstwy pasywnej, jak również potencjału tworzenia się wżerów. Zmiana fraktala powierzchni jest w dobrej zgodności z wynikami uzyskanymi dla wysokościowych współczynników chropowatości z pomiarów AFM.

1. Introduction

Austenitic stainless steel is the most popular alloy to be used as osteosynthesis plates for orthopedics applications. This popularity is due to a satisfactory combination of good mechanical and corrosion properties, as well as reasonable cost. But during exposure to physiological environments the protective surface oxide inherent to 304 is not stable [1-3]. The susceptibility of 304 stainless steel to localized corrosion in a given environment depends critically on the surface state of the alloy [4]. A protective oxide layer will form spontaneously due to contacting the steel to moist air. Coates [5] has reviewed the effects of surface treatments on corrosion characteristics of stainless steels, and concluded that mechanical treatments decrease surface roughness and therefore improve pitting resistance; however mechanical polishing may deformed the surface layer and produce residual stresses on the workpiece surface [6,7]. The electropolishing technology is a dedicated and precise polishing process. It would not only remove deformed surface layer and improve surface roughness but also form a thin passive film on the surface. This passive film, because of its metallurgical composition, will increase the corrosion resistance [8,9]. Similarly, Hultquist and Leygraf showed that all treatments (pickling, passivation or mechanical) result in chromium enrichment of the surface. They claimed that crevice corrosion resistance increases with increasing surface chromium content, whilst pitting corrosion resistance depends more strongly on the removal of surface inhomogeneities, such as inclusions [10]. The effect of surface treatment on corrosion behavior of materials was investigated [11-14]. Dick et al. [15] studied the effect of surface treatment and passivation on corrosion of stainless steel in NaCl solution and indicated that corrosion resistance was improved. Also it was shown that surface treatment was effective on corrosion behavior of implant material in physiological solution [16,17].

The objective of present work is to determine the influence of surface treatment such as mechanical, chemical and electrochemical surface preparation on the formation, stability and deterioration of surface films formed on 304 austenitic

* ABADAN FACULTY OF PETROLEUM ENGINEERING, PETROLEUM UNIVERSITY OF TECHNOLOGY, ABADAN, IRAN
** DEPARTMENT OF MATERIALS ENGINEERING, ISFAHAN UNIVERSITY OF TECHNOLOGY, ISFAHAN, IRAN

stainless steel in Tyrode physiological solution by means of AC and DC electrochemical methods.

2. Materials and procedures

The flowchart of experimental procedure is shown in Fig. 1. Test specimens were prepared from austenitic stainless steel, AISI 304, with the following chemical composition (wt %): 0.53%Si, 1.93%Mn, 17.18%Cr, 8%Ni, 1%Mo, 0.003% S and balance Fe. Specimens, having 1 cm×1 cm×4 mm dimensions were mounted in polyester resin, leaving a bare surface area of 1 cm^2 and then mechanically abraded down to1200 mesh, using emery paper. Specimens were then degreased using acetone rinsed by distilled water and finally treated as shown in Fig. 1

- The method of electropolishing (EP) conforms to ASTM E 1558-99, 250 mL water with750 mL sulfuric acid for 60 s at voltage 6 V, was used.
- Chemical passivation (CP) conforms to ASTM A 380-99, 30 Vol% HNO_3 for 20 min at temperature 60°C, was used.
- Acid cleaning (AC) according to ASTM A 380-99, 25 Vol% HNO_3 and 8 Vol% HF was used for 30 s at room temperature.
- For Ultrasonic cleaning (UC), specimens were placed in the acetone solution and cleaned using Ultrasonic Cleaners for 10 minutes at room temperature.

Corrosion tests were performed in Tyrode's physiological solution having the following composition: NaCl-8.00 g/dm^3, $NaHCO_3$-1.00 g/dm^3, KCl-0.20 g/dm^3, $CaCl_2$-0.20 g/dm^3, $MgCl_2$-0.05 g/dm^3 and Na_2HPO_4-0.05 g/dm^3 [1].

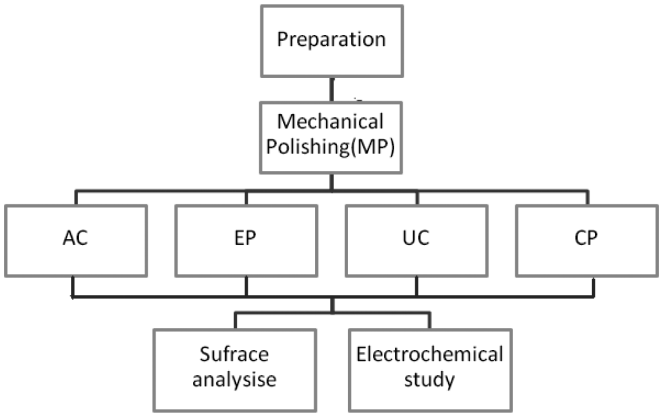

Fig. 1. Flowchart of the experimental procedure for surface treatments and corrosion investigation of 304 stainless steel implants

For more evaluation of electrochemical behavior, EIS measurement at Open Circuit Potential (OCP) was done. The frequency range used was 100 kHz – 1 mHz, with a 10 mV amplitude sine wave generated by a Frequency Response Analyzer. Polarization and impedance studies were conducted using Auto Lab Model PGSTAT 302N potentiostat/galvanostat. The scan rate used was 1 mv/sec from negative (cathodic) overpotential. The corrosion current density was obtained using Tafel extrapolation technique. Fitting of experimental impedance spectroscopy data to the proposed equivalent circuit was done by means of home written least square software based on the Marquardt method for the optimization of functions and Macdonald weighting for the real and imaginary parts of the impedance [18, 19]. A standard three electrode cell consisting of an Ag/AgCl reference, a Platinum auxiliary electrode with surface area 2 cm^2 and a working electrode (specimen) was used for corrosion test.

Scanning electron microscopy (SEM), model XL30 equiped with Energy-dispersive X-ray spectroscopy at (EDX) and AFM atomic force microscope Model Nanosurf easyS-van 2 AFM, S witzerl, were used to characterize specimens' surface before and after tests.

In this study, specimens were prepared using five different surface treatments, for every treatment at least three independent experiments were performed in order to make sure the reproducibility and standard deviations were calculated and reported.

3. Results and discussion

Cyclic potentiodynamic polarization curves of 304 SS after different surface treatments: electropolishing (EP), mecanicalpolishing (MP), chemical passivation (CP), acid cleaning (AC) and ultrasonic cleaning (UC) in Tyrode's solution are shown in Fig. 2. Experimental polarizations were done in cyclic scan but anodic and cathodic scan was separated in more clear form in Figure 2a&b. The polarization curves show Tafel type behavior of these samples. Under the condition, the main cathodic reaction is reduction of H^+. Tafel calculations are listed in Table 1&2, where E_{corr}, I_{corr}, β_a, β_c, R_p, I_{ps}, I_b, E_{pit}, E_{pp} and E_{pro} are the corrosion potential, corrosion current density, anode Tafel constant, cathode Tafel constant, polarization resistance, passive current, backward exchange current, pitting potential, primary passive potential and protective potential, respectively. Polarization resistance (R_p) values were determined from the slope of the polarization curve and calculated using Stern–Geary equation which is given below:

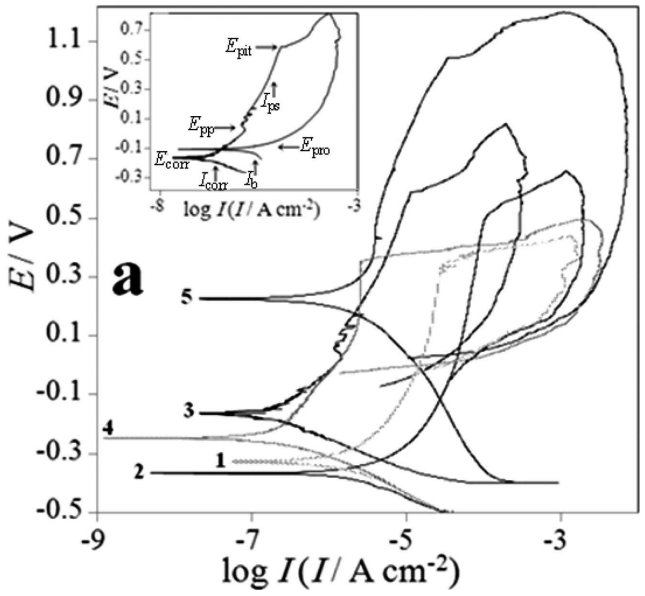

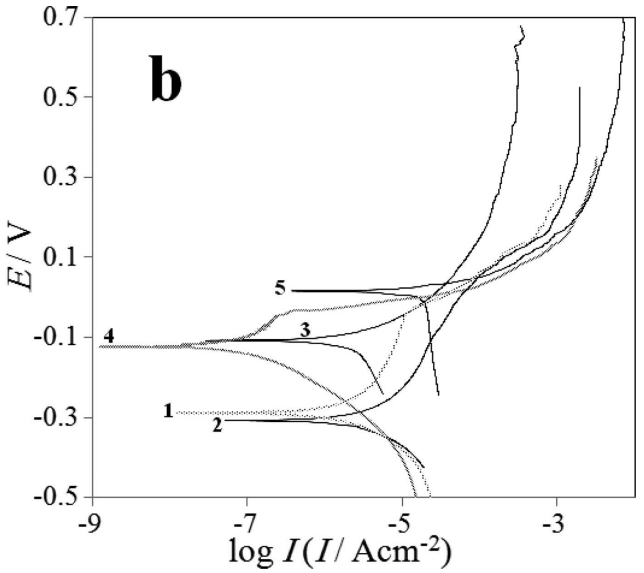

Fig. 2. Polarization curves of 304 SS obtained in Tyrode's solution, after different treatments: 1) Mechanical polishing, 2) Acid cleaning, 3) Electropolishing, 4) Ultrasonic cleaning, and 5) Chemical passivation

TABLE 1
Polarization parameters in the corrosion of 304 stainless steel in Tyrode's solution after different treatments

Treatment	$I_{corr}\times 10^7$ A cm^{-2}	β_a	β_c	R_p Ω	$I_{ps}\times 10^6$ A cm^{-2}	$I_b\times 10^6$ A cm^{-2}
MP	1.25	0.088	-0.053	11491	16.21	1.184
AC	1.41	0.075	-0.062	10452	46.77	2.57
UC	0.25	0.087	-0.051	55843	2.13	0.067
EP	0.36	0.111	-0.059	46465	2.51	1.23
CP	2.05	0.132	-0.068	9506	8.12	15.84

TABLE 2
Polarization parameters in the corrosion of 304 stainless steel in Tyrode's solution after different treatments

Treatment	E_{corr} V	E_{pit} V	E_{pro} V	E_{pp} V	$E_{pit}-E_{pp}$ V	$E_{pit}-E_{pro}$ V
MP	-0.307	0.349	-0.031	0.043	0.306	0.380
AC	-0.367	0.516	-0.026	-0.027	0.543	0.539
UC	-0.245	0.357	-0.027	0.101	0.384	0.384
EP	-0.161	0.589	-0.111	0.031	0.558	0.700
CP	0.225	1.045	0.024	0.423	0.622	1.021

Inspection of the curve reveals that the anodic scan exhibits an active/passive transition prior to a certain critical breakdown potential E_{pit}. When the critical potential E_{pit} is exceeded an increasing current is observed indicating breakdown of the passive film at local points. For $E>E_{pit}$, the current corresponds largely to the pitting corrosion of stainless steel. The increase in pitting susceptibility with increase in potential could be explained on the basis that an increase in the applied potential may increase the electric field across the passive film and therefore enhances the adsorption of the aggressive Cl^- anions on the passive electrode surface [20]. In the course of a reverse potential sweep the current decays slowly remains higher than the current in the anodic sweep and a loop characteristic of pitting corrosion phenomena, appears [20]. This loop allows the repassivation or protection potential (E_{pro}) to be determined [21]. Protection potential corresponds to the potential value below which no pitting occurs and above which pit nucleation begins [21]. When the protection potential is reached, the anodic current density decreases very sharply and rapidly. The existence of a hysteresis loop in a cyclic polarization curve indicates a delay in repassivation of an existing pit when the potential is scanned cathodically. The area of the hysteresis loop is a measure of the pit propagation kinetics. The larger the hysteresis loop the more difficult it becomes to repassivate a pit and suggest low pitting resistance [22]. As shown in Fig. 2a&b, the hysteresis loops of the specimen subjected to CP is larger than others, thereby, low pitting resistance is suggest for this treatment. The sample after UC represented smaller hysteresis loop so it has a high pitting resistance. For all treatment, the Cr content in the passive layer would increase [10]. The pit initiation after chemical passivation occurs at noble potential rather than other treatments but shows lower pitting resistance, which presents the large hysteresis loop but the passive film was unstable. Corrosion current was change in different treatment and has the order CP⟩AC⟩MP⟩EP⟩UC. As is evidence from the results presented in Fig. 2, the specimen subjected to EP shows the better corrosion resistance. This is based on noble E_{pit}, almost large passive range, small hysteresis loop, small passive current density and high polarization resistance. Ultrasonic cleaning lead to lower corrosion current and high pitting resistance (small hysteresis loop) as well as passivity region. But pitting potential and passive region for UC is lower than EP. After mechanical polishing no perfect passivation region was observed. The lower value of the I_{corr} promotes the formation of passive film, also smaller passive current density; produce the more stable passivating oxide film [22-24].

Fig. 3 shows the Nyquist diagrams of 304 stainless steel electrode recorded at open circuit potential compared the corrosion behavior of samples after electropolishing, mecanicalpolishing, chemical passivation, acid cleaning and ultrasonic cleaning in Tyrode's solution. No perfect semicircles was observed from impedance spectra obtained (Fig. 3). It was observed that Nyquist diagrams consist of two strongly overlapped capacitive semicircles which are slightly depressed towards the real axis. The depressed semicircle in the high frequency region can be related to the combination of charge transfer resistance and the double layer capacitance. The low frequency semicircle was related to resistance and capacitance of passive film on the electrode surface. The impedance data were interpreted using the equivalent electric circuit depicted in Fig. 4. To obtain a satisfactory impedance simulation of stainless steel corrosion it is necessary to replace the capacitor, C, with a constant phase element (*CPE*) Q in the equivalent circuit. The most widely accepted explanation for the emergence of *CPE* behavior, depressed semicircles, is microscopic roughness on solid electrodes causing an inhomogeneous distribution in the solution resistance as well as in the double-layer capacitance [25]. The impedance of the *CPE* is defined as $Z_{CPE} = 1/T(jw)^n$, where T is a capacitive para-

meter related to the average double layer capacitance (C_{dl}), $T = C_{dl}^{n}\left(R_s^{-1} + R_{ct}^{-1}\right)^{1-n}$ and n is a dimensionless parameter related to the constant phase angle. In equivalent electrical circuit, R_s, CPE_{dl} and R_{ct} represent solution resistance, a constant phase element corresponding to the double layer capacitance and the charge transfer resistance. CPE_f and R_f are the electrical elements related to the passive layer and with redox transformations in the passive.

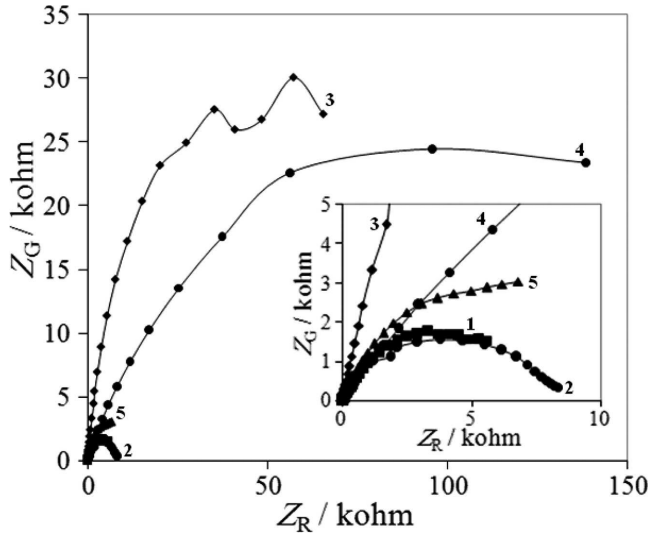

Fig. 3. EIS results a) Nyquist, b) Bode of 304 SS subjected to various surface treatment: 1) Mechanical polishing, 2) Acid cleaning, 3) Electropolishing, 4) Ultrasonic cleaning, and 5) Chemical passivation

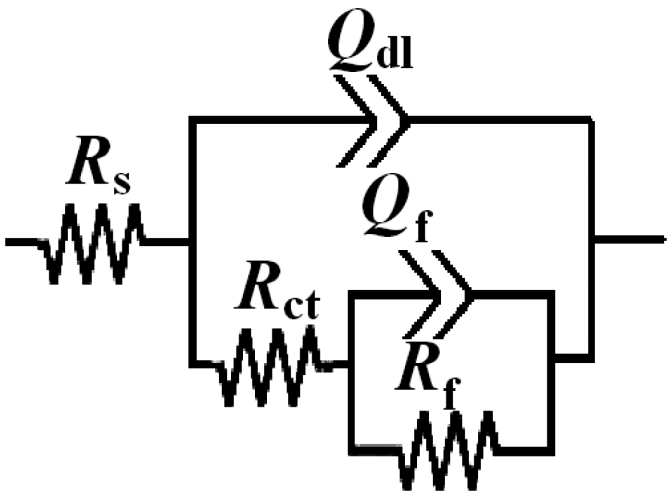

Fig. 4. Equivalent circuits compatible with the experimental impedance data in Fig. 3 for corrosion of stainless steel electrode in Tyrode's solution

The simplest approach requires the theoretical transfer function $Z(\omega)$ to be represented by:

$$Z(\omega) = R_s + \frac{R_{ct}}{\frac{1}{1+\left(Z_{pp}(\omega)/R_{ct}\right)} + (i\omega R_{ct} Q_{dl})^{n_{dl}}}$$
$$Z_{pp}(\omega) = \frac{R_f}{1+\left(i\omega R_f Q_f\right)^{n_f}} \quad (1)$$

ω is the frequency in rad/s, $\omega = 2\pi f$ and f is frequency in Hz.

To corroborate equivalent circuit the experimental data are fitted to equivalent circuit and the circuit elements are obtained. Table 3 illustrates the equivalent circuit parameters for the impedance spectra of 304 stainless steel corrosion with different pretreatment. It can be seen from Fig. 3, that higher corrosion and passive resistance was obtained for electropolished and ultrasonic cleaned sample in agreement with polarization diagrams. As the Q_{dl} exponent (n) is a measure of the surface heterogeneity, values of n indicates that the steel surface becomes more and more homogeneous. From the double layer capacitances the real electrode surface area and the relative surface roughness can be estimated, with comparison of average double layer with the value 20 μF cm^{-2} for smooth electrode according to Trasatti [26]. As can be seen EP surface has lower relative roughness parameter.

TABLE 3
Equivalent circuit parameters in the corrosion of 304 stainless steel in Tyrode's solution after different treatments

Treatment	R_s / Ω	R_{ct} / Ω	$Q_{dl}\times10^4$ / F	R_f / Ω	$Q_f\times10^5$ / F	n_{dl}	n_f
MP	18	1122	1.9	5941	7.5	0.65	0.75
AC	18	1261	2.1	7172	2	0.51	0.51
UC	17.7	7971	2	162169	8.1	0.53	0.54
EP	18.1	5487	1.1	89553	4.2	0.68	0.69
CP	18.4	1572	2.2	9169	10.5	0.68	0.78

According to these results, films obtained with electropolishing and ultrasonic cleaning present a higher resistance to the charge transfer processes, which can be associated with the highest content of chromium species in the film [6, 27, 28]. The evolution of CPE_f and of the resistance R_f with various treatment, reflect the formation of stable surface films which improves protective properties.

AFM, SEM and EDX were used to observe the surface treated profiles and surface analysis. The morphologies and surface analysis of 304 SS with different treatment are shown in Fig. 5. Furthermore, surface roughness of specimens was measured. The surface in all treatments displayed smooth and regular topography. The height roughness parameter R_a is listed in Table 4, and is defined as the mean value of the surface height relative to the center plane. The roughness of the surfaces in three different points on the surfaces was measured. Results presented in Table 4, indicate that surface roughness is reduced due to MP surface treatments. However, small variations are observed due to different surface preparations. As can be seen from EDX diagrams, higher Cr surface concentration was obtained for electropolishing surface of SS 304.

TABLE 4
Height roughness parameter and fractal dimension of surface by atomic force microscopy

Treatment	*MP*	*UC*	*EP*	*AC*	*CP*
Height roughness / nm	3.073	6.853	4.995	7.182	3.502
Fractal dimension	2.53	2.88	2.47	2.96	2.47

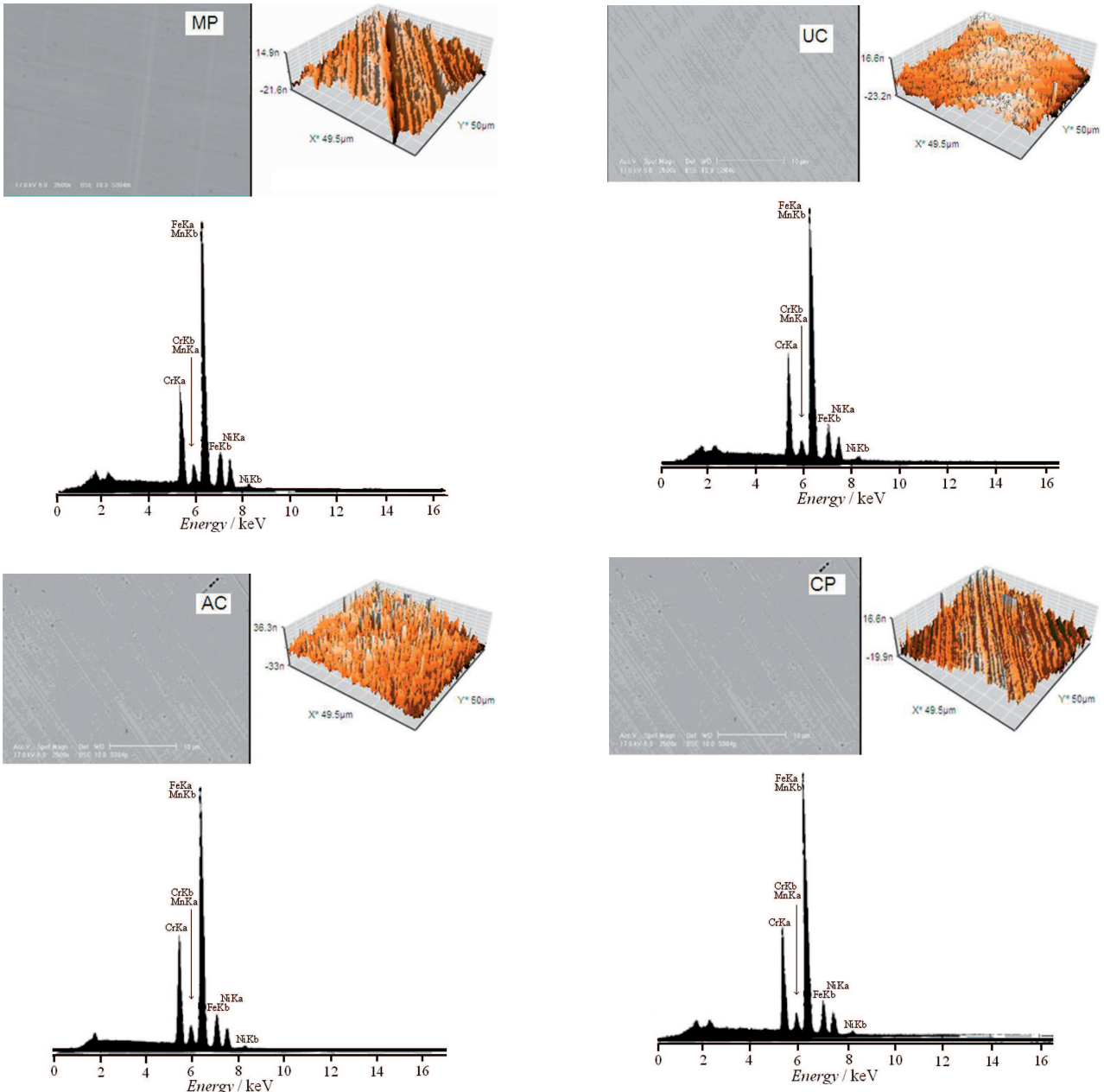

Fig. 5. Surface of steel electrode by atomic force microscopy and scanning electron microscopy (2500×) after different treatments: a) Mechanical polishing, b) Acid cleaning, c) Electropolishing, d) Ultrasonic cleaning, and e) Chemical passivation

The value of fractal dimension (D_s) can be obtained using the average of n values signifying deviation [29] from pure capacitance of a CPE in impedance measurements at different offset potentials according to the following equation [30]:

$$D_s = \frac{1}{n} + 1 \tag{2}$$

The fractal dimension of the surface, D_s, can take values between 2, for an ideally flat surface, to values less than 3 for rough surfaces. Fractal dimension of electrode surface in different treatment was presented in Table 4. Change in surface fractal is in good agreement with the result obtained from height roughness factor of AFM.

4. Conclusion

The differences in corrosion behavior of 304 stainless steel were obtained after various surface treatments according to EIS and polarization result. From the result obtained in this study following conclusion can be drawn:

- EP treatment shows the must corrosion resistance and is the most effective surface treatment.
- CP treatment shows the low pit resistance and passive film to be less protective.
- UC treatment shows a high pitting resistance.
- Acid cleaning treatment is active than respect to the MP.
- Surface roughness is reduced in MP, also small variations are observed due to different surface preparations.

As can be seen surface treatment specially electropolishing can increase the uniform and pitting corrosion resistance of implant stainless steel in physiological solution due to improving passivation and protective surface layer.

REFERENCES

[1] A. Baron, W. Simka, G. Nawrat, D. Szewieczek, Electropolishing and chemical passivation of austenitic steel, J. Achievements Mater. Manuf. Eng. **31**, 197-202 (2008).

[2] S. Ningshen, U. Kamachi Mudali, G. Amarendra, P. Gopalan, R.K. Dayal, H.S. Khatak, Hydrogen effects on the passive film formation and pitting susceptibility of nitrogen containing type 316L stainless steels, Corros. Sci. **48**, 1106-1121 (2006).

[3] T.L. Sudesh, L. Wijesinghe, D.J. Blackwood, Characterisation of passive films on 300 series stainless steels, Appl. Surf. Sci. **253**, 1006-1009 (2006).

[4] G.T. Burstein, P.C. Pistorius, Surface Roughness and the Metastable Pitting of Stainless Steel in Chloride Solutions, Corrosion **51**, 380-385 (1995).

[5] G.E. Coates, Effect of some surface treatments on corrosion of stainless steel. A review, Mater. Perform. **46**, 61-69 (1990).

[6] J.S. Noh, N.J. Laycock, W. Gao, D.B. Wells, Efects of nitric acid passivation on the pitting resistance of 316 stainless steel, Corros. Sci. **42**, 2069-2084 (2000).

[7] L. Wagner, Mechanical surface treatments on titanium, aluminum and magnesium alloys, Mater. Sci. Eng. A **263**, 210-216 (1999).

[8] S.J. Lee, J.J. Lai, The effects of electropolishing (EP) process parameters on corrosion resistance of 316L stainless steel, J. Mater. Process. Tech. **140**, 206-210 (2003).

[9] C. Charles, Jr. Irving, Electropolishing stainless steel implants, surface technology, Inc. 7, west Calhoun Memphis,TN 38103.

[10] G. Hultquist, C. Leygraf, Surface composition of a type 316 stainless steel related to initiation of crevice corrosion, Corrosion **36**, 126-131 (1980).

[11] P. Mrva, D. Kottrer, L. Kaczmarek, Arch. Metall. Mater. **56**, 743-748 (2011).

[12] D. Jedrzejczyk, M. Hajduga, Arch. Metall. Mater. **56**, 839-849 (2011).

[13] D. Jedrzejczyk, Arch. Metall. Mater. **57**, 145-154 (2012).

[14] A. Bartkowska, A. Pertek, M. Jankowiak, K. Jozwiak, Arch. Metall. Mater. **57**, 211-214 (2012).

[15] L.V. Taveira, G. Frank, H.P. Strunk, L.F.P. Dick, Corros. Sci. **47**, 757-769 (2005).

[16] M. Papakyriacou, H. Mayer, C. Pypen, H. Plenk Jr, S. Stanzl-Tschegg, Int. J. Fatigue **22**, 873-886 (2000).

[17] A. Parsapour, S.N. Khorasani, M.H. Fathi, J. Mater. Sci. Technol. **28**, 125-131 (2012).

[18] I. Danaee, S. Noori, Kinetics of the hydrogen evolution reaction on NiMn graphite modified electrode, Int. J. hydrogen energy **36**, 12102-12111 (2011).

[19] J.R. Macdonald, Note on the parameterization of the constant phase admittance element, Solid State Ion. **13**, 147-149 (1984).

[20] M. Jafarian, F. Gobal, I. Danaee, R. Biabani, M.G. Mahjani, Electrochemical studies of the pitting corrosion of tin in citric acid solution containing Cl-, Electrochim. Acta **53**, 4528-4536 (2008).

[21] Z. Szklarska-Smialowska, Pitting Corrosion of Metals, NACE, Houston, TX, 1986.

[22] E. Blasco-Tamarit, A. Igual-Muñoz, J. Garcia Antón, D. Garcia-Garcia, Effect of Temperature on The Corrosion Resistance and Pitting Behaviour of Alloy 31 in LiBr Solutions, Corros. Sci. **50**, 1848-1857 (2008).

[23] K.R. Tarantesva, V.S. Pakhomov, Pitting Resistance Criteria for Corrosion-Resistant Steels, Chem. Petrol. Eng. **45**, 412-421 (2009).

[24] K.V. Rybalka, V.S. Shaldaev, L.A. Beketaeva, A.N. Malofeeva, A.D. Davydov, Rus. Development of Pitting Corrosion of Stainless Steel 403 in Sodium Chloride Solutions, J. Electrochem. **46**, 196-204 (2010).

[25] I. Danaee, Kinetics and mechanism of palladium electrodeposition on graphite electrode by impedance and noise measurements, J. Electroanal. Chem. **662**, 415-420 (2011).

[26] S. Trasatti, O.A. Petrii, Real surface area measurements in electrochemistry, Pure Appl. Chem. **63**, 711-734 (1991).

[27] T. Hryniewicz, K. Rokosz, R. Rokicki, Electrochemical and XPS studies of AISI 316L stainless steel after electropolishing in a magnetic field, Corros. Sci. **50**, 2676-2681 (2008).

[28] L. Freire, M.J. Carmezim, M.G.S. Ferreira, M.F. Montemor, The passive behaviour of AISI 316 in alkaline media and the effect of pH: A combined electrochemical and analytical study, Electrochim. Acta **55**, 6174-6181 (2010).

[29] K.N. Jung, S.I. Pyun, Effect of pore structure on anomalous behaviour of the lithium intercalation into porous V2O5 film electrode using fractal geometry concept, Electrochim. Acta **51**, 2646-2655 (2006).

[30] G.A. McRae, M.A. Maguire, C.A. Jeffrey, D.A. Guzonas, C.A. Brown, A comparison of fractal dimensions determined from atomic force microscopy and impedance spectroscopy of anodic oxides on Zr-2.5Nb, Appl. Surf. Sci. **191**, 94-105 (2002).

Received: 20 February 2013.